

JETP 35, 1213 (1972)].

⁶L. P. Pitaevskii, Zh. Eksp. Teor. Fiz. 36, 1168 (1959) [Sov. Phys. JETP 9, 830 (1959)].

⁷V. M. Galitskii and A. B. Migdal, Zh. Eksp. Teor. Fiz. 34, 139 (1958) [Sov. Phys. JETP 7, 96 (1958)].

⁸D. Pines and P. Nozières, The Theory of Quantum Liquids, W. A. Benjamin, New York, 1966 (Russ. Transl., Mir, 1967).

⁹E. B. Osgood, V. J. Minkiewicz, T. A. Kitchens, and G. Shirane, Phys. Rev. A5, 1537 (1972).

¹⁰V. J. Minkiewicz, T. A. Kitchens, G. Shirane, and E. B. Osgood, Phys. Rev. A8, 1513 (1973).

¹¹V. Ambegaokar, J. M. Conway, and G. Baym, J. Phys. Chem. Solids Suppl. 1, 261 (1965).

Translated by A. K. Agyei.

Dopplerons and the Gantmakher-Kaner effect in tungsten plates with atomically pure surfaces

Yu. S. Ostroukhov, O. A. Panchenko, and A. A. Kharlamov

Physics Institute, Ukrainian Academy of Sciences

(Submitted November 5, 1975)

Zh. Eksp. Teor. Fiz. 70, 1838-1850 (May 1976)

The surface resistance of thin single crystal tungsten plates in the radio-frequency range is investigated as a function of the intensity of a magnetic field directed along the normal to the surface. The measurements were made on samples whose surfaces had been purified in a high vacuum (10^{-11} mm Hg) or covered with a monomolecular impurity film. The smooth variation of the real $R(H)$ and imaginary $X(H)$ components of the impedance due to the anomalous skin effect, as well as the component $R^{osc}(H)$ that oscillates with respect to magnetic field and is due to the Doppler-shifted cyclotron resonance, are studied. When the magnetic field is oriented along a fourfold symmetry axis ($\langle 100 \rangle$), resonance sets in for carriers lying on the inflection of the hole octahedron of the tungsten Fermi surface. Resonance-induced dispersion of the imaginary part of the nonlocal conductivity produces weakly damped circularly polarized transverse waves dopplerons [L. M. Fisher, O. V. Konstantinov, *et al.*, Zh. Eksp. Teor. Fiz. 60, 759 (1971) and 63, 224 (1972) [Sov. Phys. JETP 33, 410 (1971) and 36, 118 (1973)]; R. G. Chambers and V. G. Skobov, J. Phys. 1, 202 (1971); D. S. Falk *et al.*, Phys. Rev. B1, 406 (1970)]. It is found that the amplitude of the doppleron signal depends on the state of the sample and increases with increasing crystal purity. The observed changes are attributed to the increase of the specular-reflection coefficient of the resonant electrons. If the magnetic field is not normal to the plate surface, the doppleron wave undergoes collisionless magnetic Landau damping and the signal is reduced to a value comparable with the amplitude of the Gantmakher-Kaner "wave." Purification of the surface (and the ensuing increase specularity) decreases the doppleron amplitude further and produces interference peaks in the Gantmakher-Kaner "waves." The effect of surface currents due to the static skin effect, on the smoothly varying components $R(H)$ and $X(H)$ and the oscillating component $R^{osc}(H)$ of the surface resistance of the plate is discussed.

PACS numbers: 72.15.Gd, 73.25.+i

INTRODUCTION

Cyclotron damping that is shifted by the Doppler effect exerts an appreciable influence on the high-frequency properties of degenerate metals. Direct and well-investigated consequences of Doppler-shifted cyclotron resonance (DSCR) are the limited helicon-existence regions in weak magnetic fields H_0 and the onset of the Gantmakher-Kaner ratio-frequency size effect in a normal magnetic field. A recent object of investigation has been one more manifestation of DSCR, namely, low-frequency electromagnetic waves found to exist in anisotropic specially compensated conductors and to be produced if the magnetic field is near the cyclotron-damping threshold. These waves were named dopplerons.^[1-4] The doppleron modes are transverse circularly polarized waves with length quite close to the extremal displacement u_{max} of some selected group of carriers outside their cyclotron period. For this reason the doppleron wave is outwardly similar to the Gantmakher-Kaner "wave,"^[5] which is produced in the

same interval of magnetic fields or close to it.

In typical experiments, doppleron waves were excited in tin metallic plates. The magnetic field was oriented along the normal to the sample surface and coincided with a high symmetry axis of the crystal. With changing field H_0 , the wave length in the metal changed and this led to the appearance of a series of resonant absorption maxima corresponding to satisfaction of the standing-wave conditions in the plate. The impedance oscillations were observed against the background of smooth but much larger changes of the impedance, due to the anomalous skin effect. In compensated metals, these changes turn out to be quite appreciable, since the conductivity of the metal decreases without limit with increasing magnetic field, in proportion to $(\omega_c \tau)^2$, where ω_c is the cyclotron frequency and τ is the momentum relaxation time of the electrons.

In the radio-frequency band there exist thus several mechanisms responsible for energy dissipation in the plate: the anomalous skin effect, doppleron waves, and

Gantmakher-Kaner waves. The anomalous skin effect gives way to the normal one with increasing magnetic field H_0 .

It is known that the response of a metal to high-frequency excitations depends to a considerable degree on the behavior of the conduction electrons at the surface of the crystal. The influence of the character of the reflection on the impedance of compensated metals in a magnetic field directed normal to the surface ($H_0 \parallel n$) was investigated in^[6,7]. It was established that, in a wide range of frequencies and magnetic fields, when $l > r > \delta_0$ (l is the carrier mean free path, r is the Larmor radius, and δ_0 is the skin-layer depth), for diffuse scattering of the electrons ($q=1$), the impedance of bulky samples ($d \gg \delta_0$) is almost independent of the magnetic field and varies smoothly with H_0 , increasing from a constant corresponding to the anomalous skin effect in weak fields to a linear dependence corresponding to the normal skin effect in strong fields. The increase of the specularity leads to an appreciable increase of the depth of the anomalous skin layer δ_0 and of the losses in the sample. These changes are due to the static skin effect, which changes the average conductivity of the sample near its surface. In sufficiently thin plates ($d \leq \delta_0$) the mutual influence of the two skin layers on the opposite sides of the sample causes a unique size effect, wherein, the loss R , which depends on the magnetic field intensity H_0 , turns out to be maximal at a certain field value H^{\max} . The values of R^{\max} and H^{\max} depend naturally on the character of the electron reflection.

For the oscillating part of the impedance, an important role is played by the fact that the electrons moving from one surface to the other have a finite probability of returning to the initial surface without losing the cyclotron phase after specular reflection (under the condition $d \ll l$). This process increases the effective time of interaction between the wave and the conduction electrons. If there is no collisionless damping of the wave, an increase of the specularity should make the interference absorption peaks sharper. In the presence of collisionless damping (for example, when the wave vector k and the field vector H_0 are not congruent and magnetic Landau damping sets in), a competing process appears and tends to decrease the oscillation amplitude.

In situations when the radiation passing through the plate is transported only by free electrons that move along ballistic trajectories (i. e., it is due to the Gantmakher-Kaner effect) and is not connected with any propagating excitations of the electron-hole plasma of the metal (such as dopplersons), an increase of the specularity can lead to a doubling (or tripling, etc.) of the period of the size-effect oscillations of the impedance of the tin plate in terms of the magnetic field.

The phenomena listed here can be observed experimentally, since the specular-reflection coefficient depends on the surface state of the crystal. Cleaning the samples in vacuum removes the oxide film or the adsorbed foreign-matter film from the surface and bares

the true structure of the metal, which preserves the translation symmetry of the crystal lattice. Such surfaces reflect the conduction electrons with sufficient degree of specularity.^[8-11]

This paper is devoted to a comparative investigation of the high-frequency properties of thin tungsten plates with atomically-clean surface or with a surface coated with a film of adsorbed matter. The measurements were performed for a plate oriented with the (100) face, the magnetic field was directed along the normal to the surface and coincided thus with the fourfold symmetry axis (100). In this case, as was established in^[12], several dopplerson branches are observed in the tungsten crystals. The most powerful of them appears in fields 8 kOe or stronger, and is excited in "plus" polarization; it is due to the group of carriers located on the "strip" in the inflection region of the hole octahedron of the Fermi surface of tungsten (Fig. 1).

EXPERIMENTAL PROCEDURE

The quantities measured directly in the experiment were the derivative dR/dH of the real part of the impedance with respect to the magnetic field and the imaginary part $X(H)$ as functions of the magnetic field H_0 . The measurements were performed in the frequency range $f=5-10$ MHz with an installation analogous to the spectrometer used for NMR observation. The sensitivity of the autodyne oscillator was independent of the intensity H_0 in the working-field interval (0-40 kOe); this made it possible to carry out amplitude measurements of $dR/dH = F(H_0)$ in a sufficiently large range in which the Q factor of the tank circuit varied substantially.

The magnetic field was produced in a superconducting solenoid, and the value of H_0 was determined from the current I flowing through the solenoid and through a calibrated resistance Θ . The signal, proportional to the voltage $u_0 = I\Theta$, was fed to the x coordinates of an x - y recorder. The constant field was modulated in amplitude (modulation depth 300 Oe) with frequency 36 Hz. The alternating field was produced by an additional superconducting coil fed from a sound generator.

The signal from the autodyne was rectified, amplified at the modulation frequency, and fed to a phase-sensitive detector and the y coordinate of the recorder. Numerical integration of the $dR/dH = F(H_0)$ curves made it possible to obtain the dependence of the loss R on the magnetic field H_0 . The imaginary part $X(H_0)$ of the impedance was determined from the change Δf of the

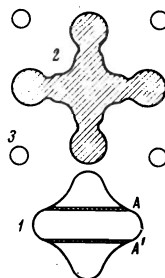


FIG. 1. Model of the Fermi surface of tungsten, section in the (100) plane. 1—Hole octahedron, 2—electron jack, 3—hole ellipsoids centered at the points N of the Brillouin zone. A and A' are the orbits of the carriers that take part in the cyclotron resonance.

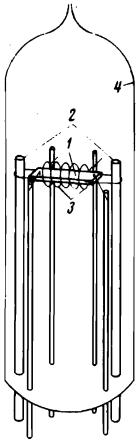


FIG. 2. Over-all view of the experimental vacuum apparatus. 1—Tungsten single-crystal plate, 2—molybdenum traverses that secure the crystal, 3—high-frequency tank-circuit inductance coil, 4—glass bulb.

autodyne tank-circuit frequency; it was assumed that $\Delta X \propto \Delta f$. The frequency was measured with a digital frequency meter feeding a printout unit.

The investigated samples were rectangular plates measuring 6×2 mm and were cut from a single-crystal block with a ratio $\rho_{300 \text{ K}} / \rho_{4.2 \text{ K}} \sim 10^5$. The estimated mean free path l in such crystals is ~ 1 mm. The plate surface was polished with corundum or diamond abrasive. The defect layer resulting from the polishing (its depth was $30\text{--}50 \mu$) was removed in a bright-dip solution. The plate thickness was monitored accurate to 1μ and ranged from 80μ to 1 mm. The accuracy of the orientation of the face was 15 minutes of angle. The axes of the plates coincided with the $\langle 100 \rangle$ crystallographic direction.

The tank-circuit coil was placed together with the sample in a glass vacuum bulk with working pressure 10^{-11} mm Hg. The bulk construction is shown in Fig. 2. The no-form high-frequency coil had a diameter 4 mm and 30 turns, and was made of tungsten wire of 200μ diameter. The investigated samples were suspended inside the coil with four thin tungsten filaments of 100μ diameter, welded to the ends of two elastic molybdenum traverses. Current flow could heat the investigated samples to temperature 2500°K . The coil could withstand a heat rise to 1000°C without distortion. The coil was heated by electron bombardment. The cathode was a thin tungsten helix. The crystals were purified in vacuum at high temperature by the standard procedure described by Stern.^[13] We note here that the tungsten crystals purified by this technology provide clearly seen diffraction patterns of slow electrons and have thus an atomically-smooth surface relief, which preserves the translational symmetry of the crystal lattice.

In the measurements, the entire vacuum tube was immersed in a helium cryostat. The thermal conductivity of the welded contacts and of the molybdenum transverse ensured cooling of the crystal to a temperature close to 4.2°K . The samples were cleaned both during the course of the many-hours' evacuation of the tube with a vacuum setup, and directly prior to the experiment with liquid helium poured in the cryostat. A "flash"—instantaneous raising of the crystal tempera-

ture—removed the adsorbed film that settled on the crystal surface from the residual-gas atmosphere. A monomolecular film (principally CO molecules) was restored within several days, after which the experiment could be carried out.

For an independent control on the sample quality and on the surface state, additional measurements were made of the static skin effect of the investigated crystals. To this end, an electric current of 1 A was passed through the crystal and the voltage drop across the crystal placed in a magnetic field $H_0 = 20$ kOe was measured.

DOPPLERONS AND THE GANTMAKHER-KANER EFFECT

Figure 3 shows plots of the derivatives dR/dH of the real part of the surface impedance with respect to the magnetic field against the applied field H_0 at the electromagnetic excitation frequency $f = 9$ MHz. The measurements were performed for a plate with $d = 85 \mu$ for the "dirty" (curve 1) and atomically-pure (curve 2) crystal surfaces. The curves were plotted at identical gains of the measurement setup.

The presented plots indicate that the observed phenomenon has all the attributes of an electromagnetic wave produced in a metal near the edge of the DSCR. Indeed, it is seen from the figure that the region in which the oscillations are observed is distinctly delineated on the weak-field side. The oscillations are almost equidistant in terms of the magnetic field; in extremely strong fields their period remains constant and coincides with the period of the Sondheimer oscillations observed in the same crystal. With changing frequency f , all the singularities of the derivatives shift in the magnetic-field scale in proportion to the cube root of their frequency. Finally, the oscillations are excited only in one circular polarization.

We assume therefore that each impedance maximum corresponds to $(S + \frac{1}{2})$ doppleron wavelengths spanned by the plate thickness at a given value of the field H_0

$$2\pi(S + \frac{1}{2}) = k(\omega, H_0)d. \quad (1)$$

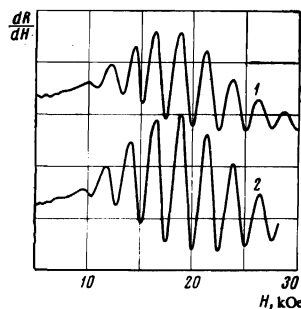


FIG. 3. Plots of the derivative of the resistance of a single-crystal tungsten plate against the constant magnetic field H . The normal to the surface of the plate and the vector \mathbf{H} are parallel to the $\langle 100 \rangle$ axis, the plate thickness is $d = 85 \mu$, and the alternating-field frequency is $f = 9$ MHz. 1—Plot for crystal with oxidized surface, 2—for crystal with atomically-pure surface.

Here S is an integer; the term $\frac{1}{2}$ is connected with the antisymmetrical character of the plate excitation. In extremely strong fields the doppleron wavenumber $k(\omega, H_0)$ tends to its asymptotic value $k_0(H)$, which satisfies the DSCR condition in the crystal:

$$\left| \frac{k_0(H)v_z}{\omega_c} \right|_{\max} = \frac{ch k_0(H)}{2\pi e H} \left| \frac{\partial A(\epsilon, p_z)}{\partial p_z} \right|_{\max} = 1, \quad (2)$$

where

$$\omega_c = \frac{eH}{m_e c}, \quad m_e = \frac{\hbar^2}{2\pi} \frac{\partial A}{\partial \epsilon}, \quad v_z = \frac{1}{\hbar} \frac{\partial \epsilon}{\partial p_z}$$

ω_c and m_e are the cyclotron frequency and the mass of the electron, v_z is the maximum velocity in the z direction, c is the speed of light, and e is the absolute value of the electron charge. The ratio v_z/m_e is expressed here in terms of the derivative of the area of the cross section of the Fermi surface $A(\epsilon, p_z)$ with respect to p_z . The value

$$L = \frac{\hbar}{2\pi} \left| \frac{\partial A(\epsilon, p_z)}{\partial p_z} \right|_{\max},$$

calculated from (1) and (2) for extremely strong magnetic fields is equal to $(0.49 \pm 0.05) \text{ \AA}^{-1}$ for a set of plates with different thicknesses and agrees well with the published data^[14-16] for extremal sections lying on the inflections of the hole octahedron of the Fermi surface of tungsten (Fig. 1). These regions produce two opposing rather strong diverging electron beams that make the principal contribution to the nonlocal conductivity of the crystal. Their focusing in the longitudinal magnetic field gives rise to two other size-effect phenomena: the Gantmakher-Kaner effect and the Sondheimer oscillations.

The main singularities of the doppleron spectrum and damping can be analyzed with a simple model as an example. We approximate the hole equal-energy surface by a corrugated cylinder whose axis is directed along the magnetic-field vector. For this case, the maximum hole-velocity v_z in the z direction is reached at an inflection point of the cylinder. Within the framework of this model, the dispersion equation is^[4]

$$k(H) = k' + ik'' = \left(-\frac{\omega_c}{v_z} + \frac{i}{l} \right) \sqrt{1 - (\omega B/H^2)^2}. \quad (3)$$

It was assumed here that $\omega_c \gg \omega$ and $\omega_c \tau \gg 1$, and that the electron conductivity is taken into account in the local limit. The constant B is equal to $4\pi N m^2 v_z^2 / e$, where N is the hole density and is equal numerically to the volume of the cylinder within the limits of the Brillouin zone. It is seen from (3) that the doppleron spectrum has no upper limit; the doppleron wavelength decreases linearly with H in a strong magnetic field, and the damping length is equal to l for the resonant carriers. It is important to note that in strong magnetic fields the spectrum and the damping of the doppleron depend exclusively on the behavior of a relatively small group of resonant carriers that lie on a narrow strip in the region of the inflection of the Fermi surface. This justifies the rather arbitrary choice of the model for the equal-energy surface.

In the interpretation of the phenomena that occur when the plate is cleaned, we shall assume that the oxi-

dized surface reflects the electrons only diffusely ($\rho = 0$). In this case, the mean free path of the resonant carriers is limited by the dimensions of the sample and the damping length of the doppleron (in thin samples with $d < l$) is equal to the plate thickness. Cleaning the surface increases ρ and the average effective wavelength l^* , and consequently also the doppleron damping length.

Thus, one of the possible causes of the increase in the signal amplitude (see the experimental curves 1 and 2 of Fig. 3) may be the increase of the coefficient of specular reflection for the resonant carriers. The shunting effect exerted on the oscillation amplitudes by the surface currents produced in the crystal because of the static skin effect will be considered later on.

When the magnetic field is deflected from the normal to the sample surface, the doppleron wave propagates at an angle to H . In this case the wave energy is transferred resonantly to the charged carriers moving with average velocity equal to the phase velocity of the wave: the wave experiences in this case collisionless magnetic Landau damping and the signal amplitude is appreciably decreased.^[17,18] The wave damping depends on the inclination of the magnetic field and manifests itself if the electron relaxation time τ is long enough. In our experiments the wave vector was always parallel to the $\langle 100 \rangle$ crystal axis, and the magnetic field made an angle Φ with the normal to the surface. The accuracy with which Φ was determined was $2-3^\circ$. The angle did not exceed 10° . Figure 4 shows a series of plots of the derivative of the real part of the surface impedance with respect to H for a crystal with $d = 195 \mu$ at an inclination angle $\Phi \approx 5^\circ$. Curve 1 was measured for a crystal with oxidized surface, curve 3 for a crystal with atomically pure surface, and curve 2 corresponded to a certain intermediate case with a submonolayer film of foreign matter on the plate surface. The surface impurity was dispensed in accordance with the exposure time in the residual-gas atmosphere and was monitored against the change of the static resistance of the crystal in a normal magnetic field $H = 20 \text{ kOe}$.^[10] Use was made here of the fact that the magnetoresistance ρ of the samples was increased 20-50% by cleaning the surface. The relative change of ρ depended on the plate thickness and on

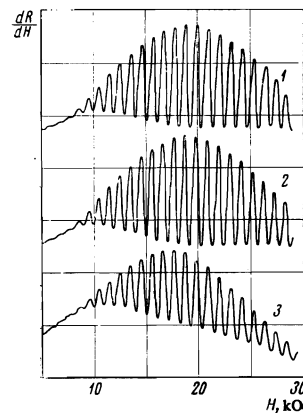


FIG. 4. Plots of the derivatives of the surface resistance of the plate against H . The normal to the sample surface coincides with the $\langle 100 \rangle$ axis. The vector H makes an angle $\Phi \approx 5^\circ$ with the normal. The plate thickness is $d = 195 \mu$ and the alternating field frequency is $f = 6 \text{ MHz}$. 1—Crystal with oxidized surface; 2—crystal with a submonolayer impurity film on the surface; 3—crystal with atomically pure surface.

the quality of the initial material. The changes were reversible and were well reproduced in each succeeding measurement cycle. The use of this device made it possible to trace all the successive stages of the oscillation-amplitude variation as a function of the state of the sample surface. It is seen from Fig. 4, for example, that a decrease in the concentration of the surface impurity (or an increase in the specularity coefficient) leads initially to a certain increase of the doppleron amplitude. Further decrease of the concentration in the adsorbed film leads to a noticeable decrease of the oscillation amplitude. The final value of the signal (for an atomically pure surface) depends thus on the inclination angle of the magnetic field and decreases with increasing Φ . The observed decrease of the amplitude following the cleaning of the crystal can be interpreted here as a result of an increase in the effective electron relaxation time τ^* , which leads to an increase of the Landau damping.

At large values of Φ , the contribution of the doppleron to the oscillating part of the impedance may turn out to be comparable with the contribution made by the Gantmakher-Kaner radio-frequency size effect. The amplitude of the size effect depends little on the inclination of the vector H . At $\Phi=0$ it is small in comparison with the Doppler wave amplitude, but can be comparable with it already at $\Phi=5-7^\circ$. Let us analyze this situation separately. By virtue of the Onsager relation, we assume that the electrons with momentum p and moving on ballistic trajectories in a medium with conductivity $\sigma_{ij}(\mathbf{k}, \omega, \mathbf{H})$, are displaced after the specular reflections in a medium with $\sigma_{ij}(-\mathbf{k}, \omega, -\mathbf{H})$, i.e., they move under identical conditions. It is therefore possible to ignore the collision with the surface and to assume that the plate "thickness" has doubled (or tripled, etc., depending on the number of specular reflections). In this case the expression for the period of the Gantmakher-Kaner oscillations can be written in the form

$$\Delta H_n = \frac{c\hbar}{en d} \left| \frac{\partial A(\epsilon, p_z)}{\partial p_z} \right|_{\max} \quad (4)$$

where n is the number of specular reflections. The contribution from each order of reflection will decrease here by a factor $p \exp\{-d/l\}$ equal to the probability of carrier drift through the plate without collisions in the volume and without loss of the cyclotron

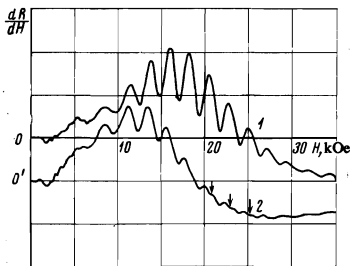


FIG. 5. Plots of the derivative of the surface resistance against H . The normal to the sample surface coincides with the $\langle 100 \rangle$ axis, the vector H makes an angle $\Phi \approx 5^\circ$ with the normal, $d=91 \mu$, $f=8$ MHz. 1—Crystal with oxidized surface, 2—with atomically pure surface. The arrows mark the additional interference maxima.

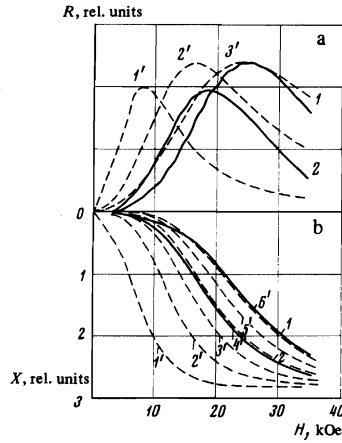


FIG. 6. Dependence of the real and imaginary parts R and X of the surface impedance on the constant magnetic field H . $d=91 \mu$, $f=8$ MHz. a) Experimental $R(H)$ plots for an oxidized (curve 1) and atomically pure (curve 2) plate surface. Curves 1', 2', and 3'—calculated plots of $R(\xi)$ with the parameter $q=0, 0.6$, and 1 , respectively. b) Experimental plots of $X(H)$ for an oxidized (curve 1) and atomically pure (curve 2) surface. Curves 1'—6'—calculated plots of $X(\xi)$ with the parameter $q=0, 0.2, 0.4, 0.6, 0.8$, and 1 , respectively.

phase at the crystal boundaries.

The doubling of the oscillation period due to the double passage of the Gantmakher-Kaner wave was observed for a thin plate ($d=91 \mu$) oriented in a magnetic field such that $\Phi \approx 5^\circ$ (Fig. 5). Curves 1 and 2 correspond to "dirty" and "clean" surfaces, respectively. The additional maxima that appear after the surface is cleaned are marked on the figure by arrows. Following the subsequent deposition of a monolayer film of adsorbed matter on the surface, the additional maxima gradually vanished and the $dR/dH=F(H)$ curve resumed its initial form.

In concluding this section we note that the specularity coefficient p for resonant electrons is limited by a certain value W_1 numerically equal to $(1 - W_2)$, where W_2 is the probability of transfer between the bands. In fact, specular reflections of resonant electrons (without loss of the cyclotron phase), correspond to transitions from the orbit A to A' (Fig. 1) with probability W_1 . At the same time, there is a finite probability of transfer between bands W_2 , with $W_2 + W_1 = 1$ and $W_1 < 1$. It is customarily assumed that in "good" metals $W_1 \sim W_2$ and consequently $p \sim 0.5$.

ANOMALOUS SKIN EFFECT

We use a numerical integration method and determine, from the experimental of $dR/dH=F(H)$ plots (Fig. 5), the dependence of the loss $R(H)$ in the sample on the applied magnetic field in explicit form. The results of the calculation are shown in Fig. 6a. Figure 6a shows the imaginary part of the impedance as a function of H for the same plate. The $X(H)$ curves were measured directly under the assumption that ΔX is proportional to the change Δf in the frequency of the tank circuit of the autodyne. The origin was assumed to correspond to the values $R(0)$ and $X(0)$ in a zero mag-

netic field. It is seen from the curves of Fig. 6 that the contribution of the oscillating part of the impedance to the general loss balance is small and the bulk of the loss is due the anomalous (in weak fields) or the normal (in strong fields) skin effect.

Let us examine the behavior of the smooth parts of $R(H)$ and $X(H)$ as functions of the applied magnetic field and of the surface quality. It is seen from the figure that the losses in the plates increase monotonically with the field, reaching a maximum at $H_0 = H^{\max}$, and decrease with further increase of the field. After cleaning the surface, the $R(H)$ and $X(H)$ curves do not change qualitatively in form but both plots (including the position of the maximum on the $R(H)$ curve) shift towards weaker fields.

In the interpretation of these phenomena we shall assume that the conductivity of the medium does not differ from its local limit and decreases in proportion to $(\omega_c \tau)^2$ with increasing magnetic field. We note here that the conductivity near the sample surface, in a layer of the order of r , depends on the character of the collisions between the carriers and the crystal boundary and coincides with the bulk conductivity (in a normal magnetic field) only in the case of purely specular reflections. Diffuse reflections increase the electron mobility along the crystal walls and bring about an additional high-frequency current that flows along the sample surface in a layer of the order of r . The parallel connection of the two high-frequency currents, "volume" (flowing in the entire skin layer δ_0 of the electric field E) and "surface"^[19] (flowing in a layer r which is small in comparison with δ_0), produces a change in the plate impedance^[6]

$$Z_s^{-1} = Z^{-1} + S. \quad (5)$$

At $q=0$ we have $S=0$; $Z_s = R_s + iX_s$; R_s and X_s are the real and imaginary parts of the surface impedance of the plate with allowance for the "surface" conductivity of the medium. If the damping depth of the field in a metal δ_0 is comparable with the sample thickness d ($\xi = \delta_0/d \sim 1$), the changes introduced into the tank circuit by the sample depend on the parameter ξ and on the method of exciting the high-frequency current. In the case of bilateral excitation symmetrical in the electric field E , the loss is maximal at $\xi = 0.46$.^[20] An increase of the field intensity H (or of δ_0) leads to mutual cancellation of the high-frequency current flowing on opposite surfaces of the sample, and to a decrease of the losses. A similar effect was observed earlier in bismuth^[20] and tin^[21,22] plates.

To compare the experimental curves with calculation, we write down the values of the real (R_s) and imaginary (X_s) parts of the impedance of a thin plate:

$$R_s = -R_\infty \frac{F(\xi) + 2R_\infty S G(\xi)}{1 + 2R_\infty S F(\xi) + 2(R_\infty S)^2 G(\xi)}, \quad (6)$$

$$X_s = -R_\infty \frac{F'(\xi)}{1 + 2R_\infty S F(\xi) + 2(R_\infty S)^2 G(\xi)}, \quad (7)$$

where

$$F(\xi) = \frac{\text{sh } \xi - \sin \xi}{\text{ch } \xi + \cos \xi}, \quad F'(\xi) = \frac{\text{sh } \xi + \sin \xi}{\text{ch } \xi + \cos \xi},$$

$$G(\xi) = \frac{\text{sh}^2 \xi + \sin^2 \xi}{(\text{ch } \xi + \cos \xi)^2}, \quad R_\infty = 4\pi c^{-1} \sqrt{\omega/2\pi\sigma}$$

are the losses in a bulky plate without allowance for S ; $S = q\sigma_0(r/l)r$, and σ_0 is the conductivity in the absence of a magnetic field. It was assumed here that $R_\infty = X_\infty$; this is valid under normal skin-effect conditions when $\delta_0 = c/\sqrt{2\pi\sigma\omega}$. The quantity $R_\infty S$ can be easily shown to be the ratio of the current j_s in the surface layer r to the volume current j_v flowing in the entire skin-effect region in the case of pure specular reflection, or to be equal to r/δ_{0n} , where δ_{0n} is the depth of the normal skin layer in the absence of a magnetic field. Estimates made for $\sigma = 10^{21} \text{ sec}^{-1}$, $f = 10^7 \text{ Hz}$ and $q = 1$ yield $\delta_{0n} \sim 1 \mu$. We assume that the value of r resulting from averaging over all the electron groups is $\sim 1 \mu$ at $H = 30 \text{ kOe}$ and increases like const/H with decreasing field. Under these conditions, the ratio j_s/j_v remains larger than or of the order of unity in the entire working interval of H , and the high-frequency current is localized in a narrow channel r near the surface. The plate impedance depends in this case essentially on the character of the electron reflection from the sample walls. This is illustrated by the family of $R(\xi)$ and $X(\xi)$ curves plotted in accordance with (6) and (7) for $\sigma_0 = 10^{21} \text{ sec}^{-1}$ and $f = 8 \text{ MHz}$ and shown dashed in Fig. 6. The parameter of the family is the quantity q that varies in the range $0 \leq q \leq 1$ in steps of 0.2. To simplify the figure the $R(\xi)$ curves are given only for $q = 0, 0.4$, and 1. It is seen from Fig. 6 that after the crystal is cleaned the $X(H)$ plot shifts towards weaker magnetic fields and is located between the two calculated $X(\xi)$ curves with parameters $q = 0.4$ and 0.6. The maximum of the absorption shifts then to a position between H^{\max} for $q = 0.4$ and 0.6.

The data on the shift of the loss maximum for the entire investigated range of frequencies f are shown in Fig. 7. The solid curves represent the calculated plots of the position of H^{\max} against the excitation frequency f for different values of the parameter q . These curves are functions of the type $H^{\max} = f^{1/2} \text{const}$. For the lower curve with parameter $q=0$ this is obvious, inasmuch as under the normal skin-effect conditions we have $R_n = 4\pi^2 c^{-2} f \delta_n$ and the losses at the maximum should be proportional only to f and d , so that (if $\delta_n = 0.46d$)

$$H^{\max} = f^{1/2} \cdot \text{const}. \quad (8)$$

The upper row of experimental points in Fig. 7 corresponds to values of H^{\max} measured for a plate with a dirty surface. The experimental points agree quite well with relation (8), thus confirming the correctness of the choice of the normal skin-effect model. Clean-

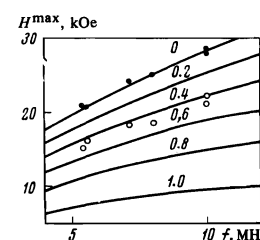


FIG. 7. Position of the magnetic-field absorption maxima for different excitation frequencies f . The points \bullet correspond to an oxidized surface and \circ to an atomically pure one. The solid curves are the calculated plots of H^{\max} against f for the set of parameters $q = 1, 0.8, 0.6, 0.4, 0.2$, and 0.

ing the crystal yields a clearly pronounced shift of the maxima towards weaker magnetic fields for all the frequencies f .

It is important to note here that for another choice of the parameters σ_0 and r , say double the initial values used in (6) and (7), the scale of the $R_s(\xi)$ and $X_s(\xi)$ curves along the ξ axis is changed. Nonetheless, the relative positions of all the singularities of these dependences, for different values of q (for example the positions of the absorption maxima), remain practically unchanged. Consequently, when the calculated curves are superimposed on the experimental ones, the errors of Δq remain within the limits of the experimental accuracy and do not influence the final result. This remark pertains equally to the curves shown in Figs. 6 and 7.

The results in Figs. 6 and 7 thus indicate that the phenomenological specular-reflection coefficient $p = (1 - q)$ estimated from the electrodynamic characteristics of a tungsten plate with an atomically pure surface is close to 0.5.

Let us estimate in conclusion the influence of the surface conductivity S (and of its variation) on the oscillating part of the plate impedance. For this purpose we generalize expression (5), including in it Z^{osc} ,

$$Z_s = \frac{Z + Z^{\text{osc}}}{1 + (Z + Z^{\text{osc}})S} \quad (9)$$

and we determine the losses for the oscillating part

$$R_s^{\text{osc}} = R^{\text{osc}} / (1 + 2RS). \quad (10)$$

It follows from (10) that the decrease of S due to cleaning the surface should increase the doppleron signal. With increasing magnetic field, this influence decreases, inasmuch as $S \rightarrow 0$ as $H \rightarrow \infty$. An analysis of the experimental data shown in Fig. 3 indicates, however, that the relative changes of the amplitude of the interference absorption maxima following cleaning the crystal surface increase with increasing magnetic field, from 20% for the first observed maximum to 80% for the last one. This allows us to conclude that the observed change of the doppleron signal is due mainly to an increase of the coefficient of the specular reflection for the resonant electrons.

The authors thank O. V. Konstantinov and V. V. Vladimirov for useful discussions and valuable advice,

and N. P. Katrich for kindly supplying the tungsten samples.

- ¹L. M. Fisher, V. V. Lavrova, V. A. Yudin, O. V. Konstantinov, and V. G. Skobov, Zh. Eksp. Teor. Fiz. **60**, 759 (1971) [Sov. Phys. JETP **33**, 410 (1971)].
- ²O. V. Konstantinov, V. G. Skobov, V. V. Lavrova, L. M. Fisher, and V. A. Yudin, Zh. Eksp. Teor. Fiz. **63**, 224 (1972) [Sov. Phys. JETP **36**, 118 (1973)].
- ³R. G. Chambers and V. G. Skobov, J. Phys. **1**, 202 (1971).
- ⁴D. S. Falk, B. Garson, and J. F. Carolan, Phys. Rev. **B1**, 406 (1970).
- ⁵V. F. Gantmakher and É. A. Kaner, Zh. Eksp. Teor. Fiz. **48**, 1572 (1965) [Sov. Phys. JETP **21**, 1053 (1965)].
- ⁶M. Ya. Azbel' and S. Ya. Rakhmanov, Zh. Eksp. Teor. Fiz. **57**, 295 (1969) [Sov. Phys. JETP **30**, 163 (1970)].
- ⁷O. V. Kirichenko, Candidate's dissertation, Khar'kov, 1974.
- ⁸A. F. Andreev, Usp. Fiz. Nauk **105**, 113 (1971) [Sov. Phys. Usp. **14**, 609 (1972)].
- ⁹P. P. Lutsishin, O. A. Panchenko, and A. A. Kharlamov, Zh. Eksp. Teor. Fiz. **64**, 2148 (1973) [Sov. Phys. JETP **37**, 1083 (1973)].
- ¹⁰O. A. Panchenko, P. P. Lutsishin, and Yu. G. Ptushinskiĭ, Zh. Eksp. Teor. Fiz. **66**, 2191 (1974) [Sov. Phys. JETP **39**, 1079 (1974)].
- ¹¹O. A. Panchenko, A. A. Kharlamov, and Yu. G. Ptushinskiĭ, Zh. Eksp. Teor. Fiz. **67**, 780 (1974) [Sov. Phys. JETP **40**, 386 (1975)].
- ¹²I. M. Bitebskiĭ, V. T. Bitchinkin, A. A. Galkin, Yu. S. Ostroukhov, O. A. Panchenko, L. T. Tsybal, and A. N. Cherkasov, Fiz. Nizkikh, Temp. **1**, 400 (1975) [Sov. J. Low Temp. Phys. **1**, 200 (1975)].
- ¹³R. M. Stern, Appl. Phys. Lett. **5**, 218 (1964).
- ¹⁴R. D. Girvan, A. V. Gold, and R. A. Phillips, J. Phys. Chem. Solids **29**, 1485 (1968).
- ¹⁵D. E. Soule and I. C. Abele, Phys. Rev. Lett. **23**, 1287 (1969).
- ¹⁶S. W. Hui and I. A. Rayne, J. Phys. Chem. **33**, 611 (1972).
- ¹⁷E. A. Kaner and V. G. Skobov, Zh. Eksp. Teor. Fiz. **46**, 1106 (1964) [Sov. Phys. JETP **19**, 749 (1964)].
- ¹⁸V. V. Lavrova, V. G. Skobov, L. M. Fisher, A. S. Chernov, and V. A. Yudin, Fiz. Tverd. Tela **15**, 2335 (1973) [Sov. Phys. Solid State **15**, 1558 (1974)].
- ¹⁹V. G. Petchanskiĭ and M. Ya. Azbel', Zh. Eksp. Teor. Fiz. **55**, 1980 (1968) [Sov. Phys. JETP **28**, 1045 (1969)].
- ²⁰H. Fischer and Y. H. Kao, Solid State Commun. **7**, 275 (1969).
- ²¹A. P. Perov, Zh. Eksp. Teor. Fiz. **63**, 1324 (1972) [Sov. Phys. JETP **36**, 699 (1973)].
- ²²I. F. Voloshin and Yu. P. Gaĭdukov, Zh. Eksp. Teor. Fiz. **67**, 334 (1974) [Sov. Phys. JETP **40**, 166 (1975)].

Translated by J. G. Adashko